

Dartmouth College

Dartmouth Digital Commons

Dartmouth Scholarship

Faculty Work

7-22-2010

The First VLBI Image of the Young, Oxygen-Rich Supernova Remnant in NGC 4449

M. F. Bietenholz
York

N. Bartel
York University

D. Milisavljevic
Dartmouth College

R. A. Fesen
Dartmouth College

Follow this and additional works at: <https://digitalcommons.dartmouth.edu/facoa>



Part of the [Stars, Interstellar Medium and the Galaxy Commons](#)

Dartmouth Digital Commons Citation

Bietenholz, M. F.; Bartel, N.; Milisavljevic, D.; and Fesen, R. A., "The First VLBI Image of the Young, Oxygen-Rich Supernova Remnant in NGC 4449" (2010). *Dartmouth Scholarship*. 1850.
<https://digitalcommons.dartmouth.edu/facoa/1850>

This Article is brought to you for free and open access by the Faculty Work at Dartmouth Digital Commons. It has been accepted for inclusion in Dartmouth Scholarship by an authorized administrator of Dartmouth Digital Commons. For more information, please contact dartmouthdigitalcommons@groups.dartmouth.edu.

The first VLBI image of the young, oxygen-rich supernova remnant in NGC 4449

M. F. Bietenholz,^{1,2*} N. Bartel,¹ D. Milisavljevic,³ R. A. Fesen,³ P. Challis⁴
and R. P. Kirshner⁴

¹Department of Physics and Astronomy, York University, Toronto, M3J 1P3, Ontario, Canada

²Hartebeesthoek Radio Observatory, PO Box 443, Krugersdorp, 1740, South Africa

³6127 Wilder Lab, Department of Physics & Astronomy, Dartmouth College, Hanover, NH 03755, USA

⁴Harvard-Smithsonian Center for Astrophysics, 60 Garden Street, Cambridge, MA 02138, USA

Accepted 2010 July 22. Received 2010 July 19; in original form 2010 May 25

ABSTRACT

We report on sensitive 1.4-GHz VLBI radio observations of the unusually luminous supernova remnant SNR 4449-1 in the galaxy NGC 4449, which gave us the first well-resolved image of this object. The remnant's radio morphology consists of two approximately parallel bright ridges, suggesting similarities to the barrel shape seen for many older Galactic supernova remnants or possibly to SN 1987A. The angular extent of the remnant is 65×40 mas, corresponding to $(3.7 \times 2.3) \times 10^{18}$ ($D/3.8$ Mpc) cm. We also present a new, high signal-to-noise ratio optical spectrum. By comparing the remnant's linear size to the maximum velocities measured from optical lines, as well as using constraints from historical images, we conclude that the supernova explosion occurred between ~ 1905 and 1961 , likely around 1940 . The age of the remnant is therefore likely ~ 70 yr. We find that SNR 4449-1's shock wave is likely still interacting with the circumstellar rather than interstellar medium.

Key words: supernovae: general – ISM: supernova remnants.

1 INTRODUCTION

In the nearby Magellanic irregular galaxy, NGC 4449, there is a remarkable object, discovered by Seaquist & Bignell (1978) in the radio. The non-thermal radio spectrum and observations of both broad and narrow optical lines (e.g. Balick & Heckman 1978; Kirshner & Blair 1980) identified the source, SNR 4449-1 (also known as 1AXG J122810+4406), as a young supernova remnant (SNR). Further work in the optical, UV and X-ray confirmed both the unusual luminosity of the object and its SNR nature (Kirshner & Blair 1980; Blair, Kirshner & Winkler 1983; Blair et al. 1984). SNR 4449-1 is quite luminous compared to known SNRs: at epoch 2000 its 1.4-GHz radio spectral luminosity (Lacey, Goss & Mizouni 2007) and the X-ray luminosity (Patnaude & Fesen 2003; Summers et al. 2003) were ~ 6 and ~ 10 times larger, respectively, than those of the ~ 330 -yr old Cas A, which is the most luminous Galactic remnant. However, in the radio as well as in the X-ray, the flux density is declining fairly rapidly, both having decreased by ~ 50 per cent over the last two decades.

Optically, SNR 4449-1 has been observed with a variety of ground-based telescopes as well as with the *Hubble Space Telescope* (*HST*), with recent results being presented in Milisavljevic &

Fesen (2008). It is situated in the northern outskirts of NGC 4449, near two prominent H II regions. Its ejecta are mainly oxygen-rich and show broad emission lines of forbidden oxygen along with both narrow H II region-like lines and broader ($v = 500$ km s⁻¹) H α and N II lines. The highest velocities are seen in the forbidden lines, whose linewidths Milisavljevic & Fesen (2008) found to be ~ 6000 km s⁻¹. The supernova type is not known, although various arguments suggest a fairly massive progenitor, with a likely mass of $\sim 25 M_{\odot}$ (see Milisavljevic & Fesen 2008, and references therein), implying that it was a core-collapse supernova (Type II or Ib,c).

The distance, D , to NGC 4449 is 3.8 ± 0.3 Mpc (Annibali et al. 2008), and we will indicate scaling with D where appropriate. The unmixed oxygen debris, high velocity and small size all point to quite a young remnant, but neither the size nor the age of the remnant has so far been well determined. Earlier very long baseline interferometry (VLBI) radio observations by de Bruyn (1983) resulted only in upper limits on the size, and it was only marginally resolved by the *HST* (Blair & Fesen 1998; Milisavljevic & Fesen 2008). Various estimates of the age have been published, from a young age range of 50–100 yr (Milisavljevic & Fesen 2008) to a rather older age of ~ 270 yr, similar to that of Cas A (Summers et al. 2003).

We have undertaken sensitive new VLBI observations using a global array in order to determine the size of the remnant and better address the questions of the remnant's age and nature.

*E-mail: mbieten@yorku.ca

2 OBSERVATIONS AND DATA REDUCTION

2.1 VLBI radio observations

We observed SNR 4449-1 on 2008 July 19, at 1.4 GHz, using the ‘High Sensitivity Array’ which consisted of nine stations of the NRAO¹ very long baseline array (VLBA) (each 25-m diameter),² and the Robert C. Byrd (~105-m diameter) as well as the Effelsberg (100-m diameter)³ telescopes. The observations lasted 12 h, and we recorded both senses of circular polarization. We used 2-bit sampling at a bit rate of 512 Mbit s⁻¹, for an effective bandwidth per polarization of 64 MHz.

The data were correlated with NRAO’s VLBA processor, and the analysis was carried out with NRAO’s Astronomical Image Processing System (AIPS). The flux density calibration was done through measurements of the system temperature at each telescope, and the antenna amplitude gains were subsequently improved through self-calibration of the reference sources. Our final data are phase-referenced to the quasar FIRST J122657.9+434058, which we will refer to as J1226+4340, and whose position of RA = 12^h26^m57^s.9044980, and Dec. = 43°40′58″.443280 (J2000) we take from the fifth VLBA calibrator survey (Kovalev et al. 2007).

2.2 Optical spectroscopy

In addition to the VLBI observations, a low-dispersion optical spectrum of SNR 4449-1 was obtained with the 6.5-m MMT telescope at Mount Hopkins in Arizona on 2008 April 1, using the Blue Channel Spectrograph (Schmidt, Weymann & Foltz 1989) with a (1 × 150) arcsec² slit and a 300 lines mm⁻¹ 4800-Å blaze grating. The slit was placed at the parallactic angle. The spectrum of the SNR was extracted using optimal extraction techniques covering a 2-arcsec region centred on the SNR and spanned the wavelength range from 3500 to 8000 Å with a full width at half-maximum (FWHM) resolution of 7 Å. Data were reduced and calibrated employing standard techniques in IRAF and standard stars from Strom (1977). No second-order filter was used, so some second-order overlap at the red end of the spectrum is possible. However, careful cross-calibration with standard stars of different colours has minimized problems this might cause in the flux calibration (see Matheson et al. 2008).

3 RESULTS

3.1 VLBI image

We show a VLBI image of SNR 4449-1 in Fig. 1. This image was obtained using natural weighting for the highest signal-to-noise ratio, and a multiscale CLEAN deconvolution (Wakker & Schwarz 1988; Greisen, Spekkens & van Moorsel 2009). We discuss the deconvolution process and the uncertainties inherent therein in more detail in Section 3.2 below. The total flux density determined from the VLBI observations was $6.5^{+1.4}_{-0.7}$ mJy, where we have estimated the uncertainty in the VLBI flux density scale as 10 per cent, and allowed an additional 20 per cent upwards uncertainty in the total flux density as it is possible that we did not recover all the extended emission

in our VLBI image. The off-source rms background brightness was 7 μJy bm⁻¹, and the peak/rms dynamic range was ~14. The FWHM of the elliptical-Gaussian convolving beam was 5.9 × 3.3 mas at -47°.

SNR 4449-1 shows a two-part radio morphology, with two bright parallel ridges of emission. Their length is 40–60 mas, and their peak-to-peak separation is ~30 mas, corresponding to $(2.3\text{--}3.4) \times 10^{18}$ (D/3.8 Mpc) cm and 1.7×10^{18} (D/3.8 Mpc) cm, respectively. The morphology might be interpreted as an elliptical shape with a deficit of brightness near the ends of the major axis, a major-axis angular diameter ~65 mas at PA ~155°, and a minor-axis one of ~30 mas. Note that the minor axis is better determined than the major one, which might be somewhat larger than 65 mas. This angular extent corresponds to $(3.7 \times 1.7) \times 10^{18}$ (D/3.8 Mpc) cm.

Our angular diameter estimate is slightly larger than the 28–37 mas estimates derived from optical *HST* measurements, where the remnant was only marginally resolved given the instrumental FWHM of 42 mas (Blair & Fesen 1998; Milisavljevic & Fesen 2008).

3.2 Imaging and deconvolution errors

The process of deconvolution can lead to errors in the image which are larger than the noise. As the signal-to-noise ratio in our image is rather low we carried out some additional tests to verify the reliability of our image.

To determine the effect of the choice of deconvolution method on the image, we tried various methods. Over the deconvolved region, the rms brightness difference between a multiscale and single-scale CLEAN image was 8 μJy bm⁻¹, and that between a maximum entropy (AIPS task VTESS) and the multiscale CLEAN image was 10 μJy bm⁻¹. These differences suggest that the deconvolution errors are between 1 and 1.5 times the rms background brightness.

One might expect a young SNR to show an edge-brightened and approximately circular structure in the radio. Could SNR 4449-1 be circularly symmetric despite the appearance of the image? In particular, it has been pointed out that some apparent deviations from circular symmetry can be due to deconvolution errors, which are coupled to the *uv* plane sampling (Heywood et al. 2009), and which tend to be bilaterally symmetric, much like the structure observed in SNR 4449-1. Could this be the origin of the observed bilateral structure? To test this possibility, we produced model visibilities from a simple, circularly symmetric shell model of an SNR chosen to approximately match SNR 4449-1 in size and location, with a total flux density of 6 mJy and random noise added at a level comparable to that in our observed visibilities. The specific model used was the projection of a 3D shell of uniform emissivity, with an outer angular radius of 28.2 mas, and an inner radius being 80 per cent of the outer one. Such a model was found to be appropriate for the supernova SN 1993J in M81 (Bietenholz, Bartel & Rupen 2003). When deconvolved, these model data produced a very circular image with a fairly uniform brightness around the rim, suggesting that the distortions seen in the image of SNR 4449-1 are not due to deconvolution errors or gaps in *uv* coverage, but are intrinsic to the source. In summary, our tests confirm that the source structure in our VLBI image is reliable, and suggest that if SNR 4449-1 has a shell morphology, it must be fairly distorted.

3.3 Optical spectrum

In Fig. 2, we show our 2008 April optical spectrum of SNR 4449-1, with the listed wavelengths given in the rest-frame of the supernova as measured by Hα emission observed at 6567 Å

¹ The National Radio Astronomy Observatory, NRAO, is a facility of the National Science Foundation operated under cooperative agreement by Associated Universities, Inc.

² The antenna at Fort Davis, Texas did not take part in this project.

³ The telescope at Effelsberg is operated by the Max-Planck-Institut für Radioastronomie in Bonn, Germany.

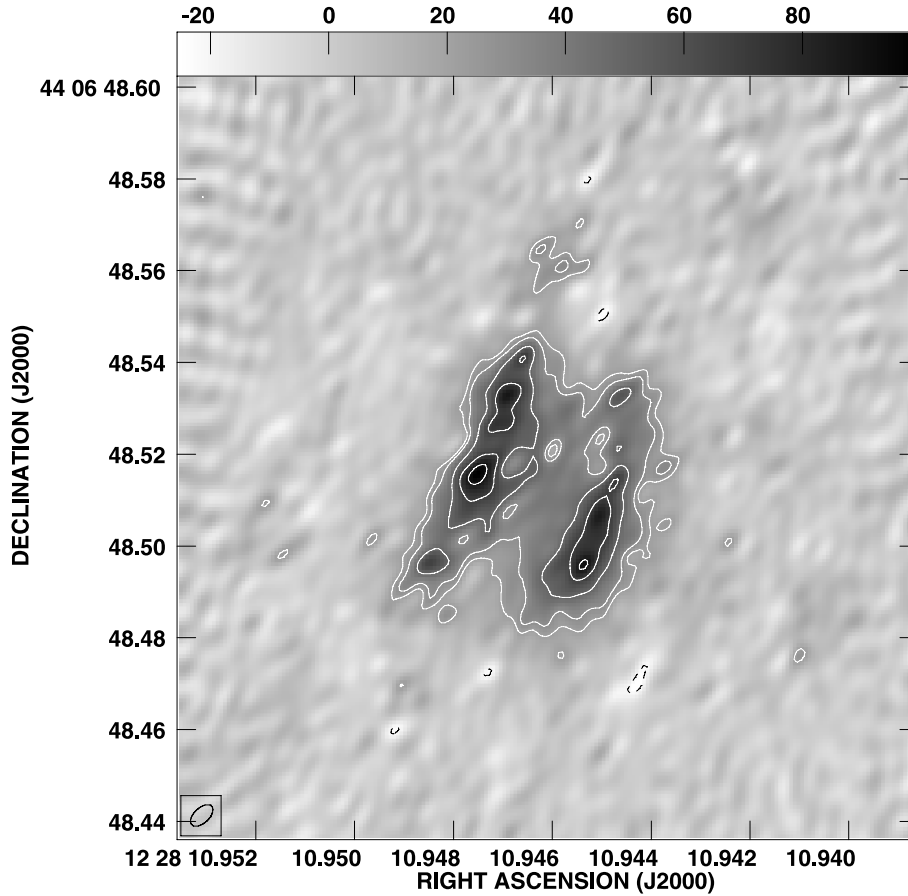


Figure 1. A 1.44-GHz VLBI image of SNR 4449-1. The contours are drawn at -22 , 22 , 30 , 50 , 70 and 90 per cent of the peak brightness, which was $98 \mu\text{Jy bm}^{-1}$. The lowest contour is three times the off-source brightness rms, which was $7.1 \mu\text{Jy bm}^{-1}$, although we estimate that the effective on-source rms is likely ~ 50 per cent higher. The FWHM of the convolving beam was $5.9 \times 3.3 \text{ mas}$ at -47° , and is indicated at lower left. The image was deconvolved using multiresolution CLEAN.

(velocity = 190 km s^{-1}) originating from a neighbouring H II region (see fig. 2 in Milisavljevic & Fesen 2008). A blue continuum likely associated with a bright star cluster is clearly visible in *HST* images (Milisavljevic & Fesen 2008) and has been subtracted.

Dominating the spectrum of SNR 4449-1 are broad [O I] $\lambda\lambda 6300$, 6364 , [O II] $\lambda\lambda 7319$, 7330 , [O III] $\lambda\lambda 4959$, 5007 emission lines consistent with the O-rich ejecta of a young SNR. Less prominent and not as broad are emission lines from [S II] $\lambda\lambda 4069$, 4076 and $\lambda\lambda 6716$, 6731 , [Ne III] $\lambda 3869$ and [Ar III] $\lambda 7136$. Contributions from nearby H II regions are also observed as narrow lines of H α , [N II] $\lambda\lambda 6548$, 6583 and [S II] $\lambda\lambda 6716$, 6731 .

In most regards, our spectrum shows no significant changes in the emission lines from the 2002 and 2007 spectra presented in Milisavljevic & Fesen (2008). However, our broader wavelength coverage and improved signal-to-noise ratio reveal some previously unreported features in the remnant's optical emission. For example, faint and broad emission centred around 7770 \AA is now seen. This emission's velocity width and line profile shape match those of the forbidden oxygen lines, and it is thus likely associated with O I $\lambda 7774$. Faint and broad emission is also observed around a narrowly peaked O I $\lambda 5577$ line. While the narrow emission may in part be an artefact of poor night sky subtraction, the underlying broad emission is likely real and associated with the remnant.

The increased sensitivity of the MMT spectra also allows for improved estimates of expansion velocities of the optically emit-

ting material. Measured from the half width at zero intensity along the red wing of the [O III] $\lambda 5007$ line, we estimate an expansion velocity of $\approx 6500 \text{ km s}^{-1}$. This velocity is marginally larger than the 6000 km s^{-1} value reported by Milisavljevic & Fesen (2008). In addition, the broad emission centred around H α can now be seen to extend from 6525 to 6605 \AA , which is 20-\AA larger than that cited by Milisavljevic & Fesen (2008) and implies expansion velocities up to $\sim 1000 \text{ km s}^{-1}$ for the H α and [N II] $\lambda\lambda 6548$, 6583 lines.

A relatively strong and broad emission feature, the so-called 'blue Wolf-Rayet (WR) bump' centred between 4600 and 4700 \AA and associated with the N III $\lambda\lambda 4634$, 4642 , N V $\lambda\lambda 4605$, 4622 , and C III/C IV $\lambda\lambda 4650$, 4658 lines, can also be seen in the spectrum, indicating the presence of WR stars of the WN type. This WR emission feature was previously seen in both ground-based and *HST* spectra and is likely from a WR population located within the OB star cluster coincident with the SNR (Milisavljevic & Fesen 2008).

Broad emission spanning $5740\text{--}6100 \text{ \AA}$ is also present with an unidentified peak around 5816 \AA . The overall position, broadness and strength resembles the 'yellow WR bump' due to C III 5696 , C IV $\lambda\lambda 5801$, 5812 and He I $\lambda 5876$ emission lines seen in the spectra of WR stars mainly of the WC type. The fact that this emission feature was not reported previously may indicate that our particular long-slit position detected neighbouring WC stars not located within the OB star cluster coincident with SNR 4449-1.

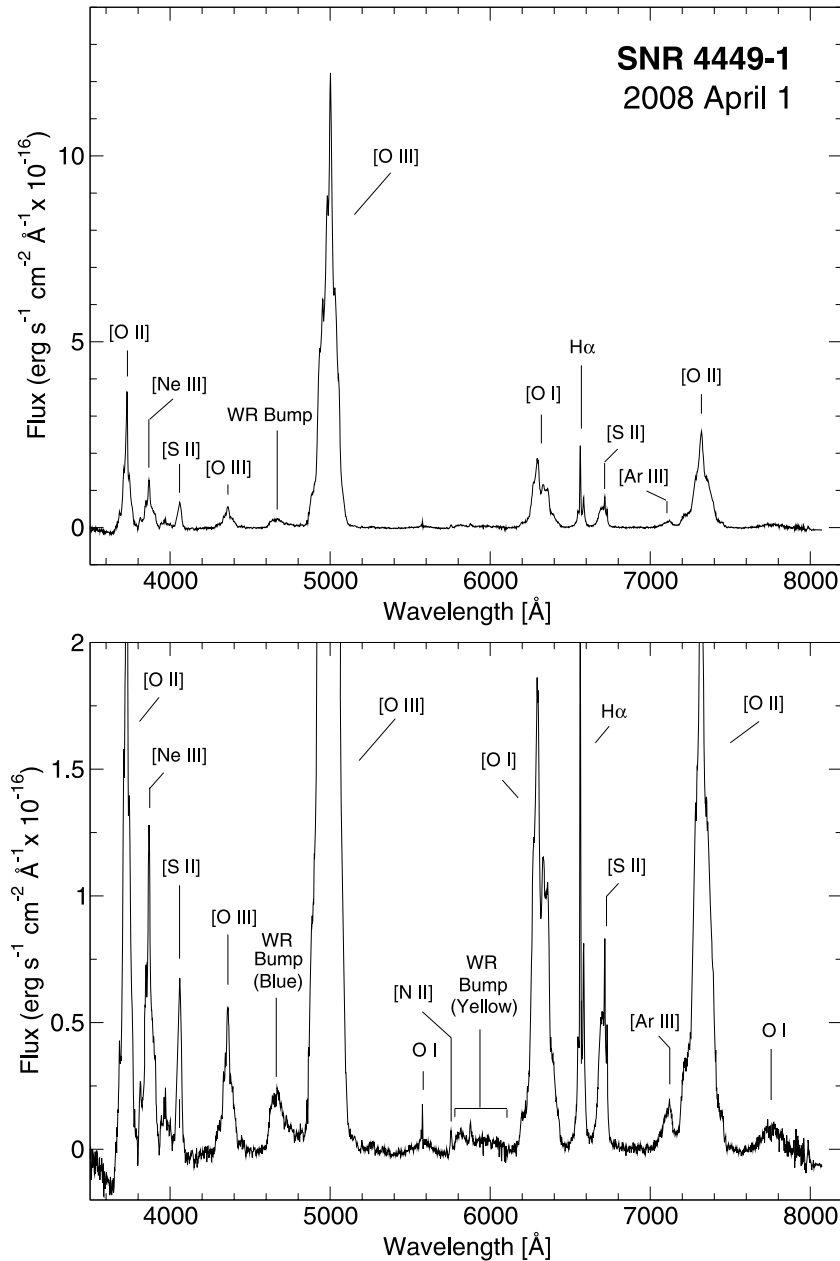


Figure 2. April 2008 optical spectrum of SNR 4449-1. The entire spectrum is shown in the top panel, with a magnified plot presented in the bottom panel to show the remnant's weaker emission features.

4 DISCUSSION

We have produced the first VLBI image of the unusually bright young SNR, SNR 4449-1, in the galaxy NGC 4449. The morphology of the remnant does not correspond to a circularly symmetric shell as might be expected for a young supernova or SNR. Instead, our VLBI image (Fig. 1) shows a two-part morphology with two parallel, almost straight ridges of emission. The overall emission region is somewhat elongated, extending over a region of about 65×40 mas, corresponding to $(3.7 \times 2.3) \times 10^{18}$ ($D/3.8$ Mpc) cm (see Section 3.1). We will discuss the morphology more extensively below, but first we turn to estimating SNR 4449-1's age, which has so far been an outstanding question.

Based on the presence of SNR 4449-1 in images from 1961, the remnant must at present (2010) be at least 49-yr old

(Milisavljevic & Fesen 2008). An upper limit on its age, however, is much less certain, with Milisavljevic & Fesen (2008) estimating $\lesssim 100$ yr while Summers et al. 2003 suggest it could be as old as ~ 270 yr.

From the [O III] line emission in our optical spectrum, we find a maximum expansion velocity of 6500 km s^{-1} . An estimate of the remnant's age can be obtained by dividing remnant's radius, determined from the VLBI image, by the maximum expansion velocity. This estimate involves a number of assumptions, whose effect on the age estimate we discuss below. First it assumes constant velocity expansion or, in practice, no significant deceleration, since acceleration is physically unlikely. Secondly, it assumes that SNR 4449-1's O-rich material is (approximately) co-located with the bright radio shell detected in the VLBI image. Thirdly, it assumes that the remnant's extent along the line of sight, or the z -direction, can be

estimated from the angular extent in the sky plane as revealed by the VLBI image.

In particular, we estimate a range of possible z -axis extents by taking the major and minor axis angular extents from the VLBI image coupled, respectively, with the 2σ range of distance estimates of 4.4 and 3.2 Mpc, giving a range of z -axis linear diameters of $(4.3\text{--}1.9) \times 10^{18}$ cm. The velocity of 6500 km s^{-1} then implies a range of ages (from the epoch of the VLBI observations of 2008.6) of 104–47 yr, or an explosion epoch between 1905 to 1962, with a median value of 1934. We note that in view of the unusual morphology of the remnant, it is possible that the extent along the line of sight could be either larger or smaller than our range, resulting in either an expansion age which could possibly be outside the range we give, but we give other arguments which limit the range of possible explosion dates below.

This process of comparing the optical expansion velocity to the size determined from the VLBI image is likely to *overestimate* the true age for two reasons. First, the remnant's outer shock front, which corresponds approximately to the outer edge of the radio emission, is likely outside of the bulk of the ejecta, and is thus moving more rapidly than the [O III] emitting gas. However, the highest velocity optical emission has been convincingly shown to have velocities close to (although slightly smaller than) that of the forward shock for SN 1993J (Bartel et al. 2007) and SN 1979C (Bartel & Bietenholz 2003). Secondly, the object's considerable and long-lived luminosity suggests a strong interaction with the local circumstellar medium (CSM), leading to the conclusion that some deceleration of the shock front and ejecta is certain to have occurred. The most likely value of the explosion epoch, therefore, is somewhat later than our median value of 1934, and we adopt a round value of 1940.

Our lower limit on the explosion epoch of 1905 is therefore conservative. In fact, as argued by Milisavljevic & Fesen (2008), it was probably later than 1913, because SNR 4449-1 is not clearly distinguishable on a deep, blue-sensitive plate from that year and would be expected to have been quite bright if it had exploded before then.

If SNR 4449-1 had undergone strong deceleration, such as SN 1987A (e.g. Gaensler et al. 1997), it could have exploded even later than 1963. However, the 1961 detection mentioned above proves that it must in fact have exploded before 1961, and we can conclude that no very strong deceleration has occurred.

We can therefore say that SNR 4449-1 most likely exploded around 1940, almost certainly between 1905 and 1961. In other words, SNR 4449-1's age is likely ~ 70 yr, which is near the middle of the range estimated by Milisavljevic & Fesen (2008). This young age makes SNR 4449-1 a very interesting case, since the youngest known Galactic SNRs are, Cas A with an age of ~ 330 yr and SNR G001.9+00.3, thought to be about 150 yr old (Reynolds et al. 2008; Green et al. 2008).⁴

Radio emission from the remnant of a high-mass progenitor should decline with time while the ejecta are interacting with the progenitor's dense stellar wind, whose density decreases approximately with the inverse square of the radius. This appears to be the case with SNR 4449-1, whose radio light curve has shown a steady decline since at least 1970 (Lacey et al. 2007). We find that the observed 1.4-GHz light curve is consistent with a continuous de-

cline with time as approximately $t^{-1.7}$ (average value between 1980 and the present, assuming an explosion date of 1940) and that the total flux density from our recent VLBI observations of $6.5^{+1.4}_{-0.7}$ mJy lies almost exactly on the extrapolation of Lacey et al.'s 1.4-GHz radio light curve. The remnant's present shock radius of $\sim 1.5 \times 10^{18}$ cm is comparable to the size of the wind bubbles around massive stars. There is no sign of any increase in the radio light curve which might suggest that the shock had encountered the interstellar medium (ISM) where the density is independent of the radius. The progression of the shock from the CSM to the ISM, which for typical remnants occurs at age of order 100 yr, should result in the flux density increasing relatively rapidly until the swept-up mass becomes roughly equal to the ejecta mass (e.g. Cowsik & Sarkar 1984). We can compare the radio luminosity of SNR 4449-1 with that of other young supernovae (SNe) and SNRs of similar age. SNR 4449-1's present 1.4-GHz spectral luminosity is $1.1 \times 10^{26} (D/3.8 \text{ Mpc})^2 \text{ erg s}^{-1} \text{ Hz}^{-1}$. Only two optically identified SNe of comparable age that have been detected in the radio: SN 1923A and SN 1950B, which have spectral luminosities of ~ 5 and ~ 13 per cent, respectively, that of SNR 4449-1 (Eck, Cowan & Branch 2002). Extrapolating their 1.4-GHz light curves of some of the more radio luminous SNe detected in the last few decades to $t = 70$ yr, we find that most are considerably fainter than SNR 4449-1. Even a luminous and long-lived example like SN 1986J has an extrapolated 1.4-GHz luminosity only 11 per cent that of SNR 4449-1 (Bietenholz, Bartel & Rupen 2010). Of the optically detected SNe, only SN 1979C, which has shown a relatively shallow flux density decay, has an extrapolated 1.4-GHz luminosity larger than SNR 4449-1, being $\sim 3 \times$ that of SNR 4449-1 (Bartel & Bietenholz 2008). The most luminous example is SN 1982aa, the radio supernova in Mrk 297 (not optically detected) which was likely a type II, which has an extrapolated 1.4-GHz luminosity of $\sim 30 \times$ that of SNR 4449-1 (Yin 1994). In other words, the radio luminosity of SNR 4449-1 is high compared to that of most SNe at age 70 yr, and even compared to that of the subset of SNe detected in the radio, but is lower than the most luminous known examples. The high luminosity suggests a dense CSM and therefore that the progenitor underwent a phase of high mass-loss phase in the period leading up to the supernova explosion.

The progenitor of SNR 4449-1 was likely quite massive. Milisavljevic & Fesen (2008) discuss the nature of the progenitor on the basis of the spectrum and the cluster turn-off, and conclude that SNR 4449-1's progenitor likely had a mass $\gtrsim 20 M_{\odot}$. They favour a luminous blue variable (LBV) over a WR star, because WR stars typically do not have a CSM dense enough to reproduce the optical spectrum of SNR 4449-1. The high and long-lived radio luminosity also requires strong interaction with a dense CSM, therefore supporting the LBV hypothesis. We conclude that SNR 4449-1 likely exploded as an LBV, or perhaps as a red supergiant.

There is no sign in SNR 4449-1 of a central radio component, such as might be associated with the neutron star or black hole compact remnant of the supernova. For example, a young and energetic pulsar might be expected to produce a very bright wind nebula. Such a central component is seen in SN 1986J, although its association with the compact remnant is not certain (Bietenholz et al. 2010). A central component has not so far been seen in any other young supernova (Bartel & Bietenholz 2005). If we take the observed peak brightness in SNR 4449-1's central region of $53 \mu\text{Jy bm}^{-1}$ as a limit, then we can say that the 1.4-GHz spectral luminosity of any unresolved central source in SNR 4449-1 must be $\lesssim 1.3 \times 10^{24} \text{ erg s}^{-1} \text{ Hz}^{-1}$ or $\lesssim 20$ per cent that of the Crab nebula.

⁴ We note also GAL 000.570–00.018 (G0.570–0.018), whose nature is uncertain, but if interpreted as an SNR, probably has an age of 80–160 yr (Renaud et al. 2006).

As we have noted, the observed morphology of SNR 4449-1 (Fig. 1) is somewhat different than that seen in the small sample of resolved radio SNe (see, e.g. Bietenholz 2008, 2005). How can it be interpreted? SNR 4449-1's observed morphology is similar to the barrel shape seen in some older Galactic SNRs (Kesteven & Caswell 1987; Gaensler 1998), which is thought to be due to interaction with the large-scale Galactic magnetic field, with the symmetry axis being preferentially parallel to the Galactic plane (Gaensler 1998). In the case of SNR 4449-1, which as we have shown is interacting with the CSM still, the influence of NGC 4449's large-scale galactic field is likely to be small, especially given the fact that SNR 4449-1 is over an order of magnitude smaller than the barrel-shaped Galactic SNRs. We do note, however, that SNR 4449-1's axis of (approximate) symmetry is also parallel to the large-scale field, which has an orientation of $\sim 45^\circ$ at the location of SNR 4449-1 (Chyży et al. 2000a,b, note that NGC 4449's magnetic field seems not to be aligned with the spiral arms as is usually the case).

The morphology of SNR 4449-1 is perhaps also reminiscent of the morphology seen in the radio for SN 1987A, which shows a ring-like structure with a prominent hotspot on either side (e.g. Ng et al. 2008; Potter et al. 2009; Tingay et al. 2009; Zanardo et al. 2010). In SN 1987A, this structure is thought to be due to the radio emission arising in a thick equatorial belt, thought to have been generated by the collision of a fast wind produced by the progenitor in its final blue supergiant stage with the slow wind from the preceding red supergiant stage (Chevalier 1988). This mechanism, however, does not seem applicable for SNR 4449-1, which must have exploded directly after a period of intense mass loss, as only interaction with a slow dense wind can give rise to SNR 4449-1's high radio luminosity which is several orders of magnitude above that of SN 1987A.

Finally, we note that the two-part morphology of SNR 4449-1 is also somewhat reminiscent of 41.95+575, the brightest and most compact radio source in M82 (e.g. McDonald et al. 2001b; Bartel et al. 1987). Although the unusual morphology of 41.95+575 has led some authors to question whether it is in fact supernova-related, it seems that on the balance the likeliest explanation is still that 41.95+575 is a supernova in a very dense environment. Its age is not known, but must be at least ~ 40 yr, with the low expansion velocity suggesting an age of ~ 75 yr, quite comparable to SNR 4449-1. Likely, 41.95+575 exploded in an even denser environment, since its radio luminosity is about 5 times higher, its rate of flux density decay about twice and its expansion speed about half those, respectively, of SNR 4449-1. On the basis of this evidence, it would seem reasonable to suppose that 41.95+575 is interacting with a particularly dense ISM, while SNR 4449-1 is at an earlier stage of its evolution and is still interacting with its CSM. Although difficult, VLBI observations of higher sensitivity would be useful to clarify the morphology of SNR 4449-1, and should be feasible with the planned increases in bandwidth for the VLBA (Uvestad et al. 2010).

5 SUMMARY

We report on high-sensitivity array VLBI observations and a high signal-to-noise ratio optical spectrum of SNR 4449-1 in the galaxy NGC 4449. Our VLBI image shows, for the first time, the morphology of SNR 4449-1, which consists of two parallel bright ridges. The morphology suggests a barrel shape, as is seen in many Galactic SNRs, or perhaps a ring shape, similar to that seen in SN 1987A. From the image, we determine also the first direct measurement of

the size of the remnant, with the extent (in the sky plane) being $(3.7 \times 2.3) \times 10^{18}$ ($D/3.8$ Mpc) cm. This extent, when combined with the velocities obtained from the optical spectrum, allows us to deduce an explosion epoch between ~ 1905 and 1961 , with a likely value near 1940 , or a present age of 70 yr. We also conclude that SNR 4449-1 is probably still interacting with its CSM.

ACKNOWLEDGMENTS

The optical observations reported here were obtained at the MMT Observatory, a joint facility of the Smithsonian Institution and the University of Arizona. Supernova studies at the Harvard College Observatory are supported by NSF grant AST09-07903, and at York University by NSERC.

REFERENCES

- Annibali F., Aloisi A., Mack J., Tosi M., van der Marel R. P., Angeretti L., Leitherer C., Sirianni M., 2008, *AJ*, 135, 1900
 Balick B., Heckman T., 1978, *ApJ*, 226, L7
 Bartel N., Bietenholz M. F., 2003, *ApJ*, 591, 301
 Bartel N., Bietenholz M. F., 2005, *Advances Space Res.*, 35, 1057
 Bartel N., Bietenholz M. F., 2008, *ApJ*, 682, 1065
 Bartel N. et al., 1987, *ApJ*, 323, 505
 Bartel N., Bietenholz M. F., Rupen M. P., Dwarkadas V. V., 2007, *ApJ*, 668, 924
 Bietenholz M., 2005, in Romney J., Reid M., eds, *ASP Conf. Ser. Vol. 340, Future Directions in High Resolution Astronomy Imaging of Radio Supernovae*. Astron. Soc. Pac., San Francisco, p. 286
 Bietenholz M., 2008, in *Supernova VLBI*, Paper 64, The Role of VLBI in the Golden Age for Radio Astronomy, <http://pos.sissa.it/cgi-bin/reader/conf.cgi?confid=72>
 Bietenholz M. F., Bartel N., Rupen M. P., 2003, *ApJ*, 597, 374
 Bietenholz M. F., Bartel N., Rupen M. P., 2010, *ApJ*, 712, 1057
 Blair W. P., Fesen R. A., 1998, *BAAS*, 30, 1365
 Blair W. P., Kirshner R. P., Winkler P. F., Jr, 1983, *ApJ*, 272, 84
 Blair W. P., Raymond J. C., Gull T. R., Fesen R. A., 1984, *ApJ*, 279, 708
 Chevalier R. A., 1988, *Nat*, 332, 514
 Chyży K. T., Beck R., Kohle S., Klein U., Urbanik M., 2000a, *A&A*, 355, 128
 Chyży K. T., Beck R., Kohle S., Klein U., Urbanik M., 2000b, *A&A*, 356, 757
 Cowsik R., Sarkar S., 1984, *MNRAS*, 207, 745
 de Bruyn A. G., 1983, *A&A*, 119, 301
 Eck C. R., Cowan J. J., Branch D., 2002, *ApJ*, 573, 306
 Gaensler B. M., 1998, *ApJ*, 493, 781
 Gaensler B. M., Manchester R. N., Staveley-Smith L., Tzioumis A. K., Reynolds J. E., Kesteven M. J., 1997, *ApJ*, 479, 845
 Green D. A., Reynolds S. P., Borkowski K. J., Hwang U., Harrus I., Petre R., 2008, *MNRAS*, 387, L54
 Greisen E. W., Spekkens K., van Moorsel G. A., 2009, *AJ*, 137, 4718
 Heywood I., Blundell K. M., Klöckner H.-R., Beasley A. J., 2009, *MNRAS*, 392, 855
 Kesteven M. J., Caswell J. L., 1987, *A&A*, 183, 118
 Kirshner R. P., Blair W. P., 1980, *ApJ*, 236, 135
 Kovalev Y. Y., Petrov L., Fomalont E. B., Gordon D., 2007, *AJ*, 133, 1236
 Lacey C. K., Goss W. M., Mizouni L. K., 2007, *AJ*, 133, 2156
 McDonald A. R., Muxlow T. W. B., Pedlar A., Garrett M. A., Wills K. A., Garrington S. T., Diamond P. J., Wilkinson P. N., 2001, *MNRAS*, 322, 100
 Matheson T. et al., 2008, *AJ*, 135, 1598
 Milisavljevic D., Fesen R. A., 2008, *ApJ*, 677, 306
 Ng C., Gaensler B. M., Staveley-Smith L., Manchester R. N., Kesteven M. J., Ball L., Tzioumis A. K., 2008, *ApJ*, 684, 481
 Patnaude D. J., Fesen R. A., 2003, *ApJ*, 587, 221

- Potter T. M. et al., 2009, *ApJ*, 705, 261
- Renaud M., Paron S., Terrier R., Lebrun F., Dubner G., Giacani E., Bykov A. M., 2006, *ApJ*, 638, 220
- Reynolds S. P., Borkowski K. J., Green D. A., Hwang U., Harrus I., Petre R., 2008, *ApJ*, 680, L41
- Schmidt G. D., Weymann R. J., Foltz C. B., 1989, *PASP*, 101, 713
- Seaquist E. R., Bignell R. C., 1978, *ApJ*, 226, L5
- Strom K. M., 1977, Kitt Peak Observatory Memorandum: Standard Stars for Intensified Image Dissector Scanner Observations
- Summers L. K., Stevens I. R., Strickland D. K., Heckman T. M., 2003, *MNRAS*, 342, 690
- Tingay S. et al., 2009, in 8th International e-VLBI Workshop, Paper 100, An e-VLBI Image of SN1987A from Australian Radio Telescopes and the JIVE Correlator, <http://pos.sissa.it/cgi-bin/reader/conf.cgi?confid=82>
- Ulvestad J. S., Romney J. D., Briske W. F., Deller A. T., Walker R. C., Durand S. J., 2010, *BAAS*, 41, 407
- Wakker B. P., Schwarz U. J., 1988, *A&A*, 200, 312
- Yin Q. F., 1994, *ApJ*, 420, 152
- Zanardo G. et al., 2010, *ApJ*, 710, 1515

This paper has been typeset from a \TeX/L\AA\TeX file prepared by the author.